Observing the Sun: from start to finish.

PhD dissertation by

Pablo Santamarina Guerrero

Instituto de Astrofísica de Andalucia (IAA-CSIC)

Programa de Doctorado en Física y Matemáticas (FisyMat)
Universidad de Granada

A thesis submitted in fulfillment
of the requirements of the degree of
Doctor of Philosophy

June 13, 2024

PhD thesis supervised by

Dr. David Orozco Suárez

Dr. Julián Blanco Rodríguez

Acknowledgements

Agradecimientos

Resumen

Resumen de la tesis

Summary

Summary of the thesis

Contents

Chapter 1

TuMag's design and calibration.

In this chapter we take the first steps of the journey of developing an instrument to observe the Sun. We will define...

The SUNRISE III mission aims to study and stablish the relations and couplings between the phenomena ocurring at different layers of the Sun's surface. With this purpose in mind, three different post-focal instruments were included in the design, each of them responsible of observing at different regions of the spectrum. The SUNRISE UV Spectropolarimeter and Imager (SUSI, **REFERENCIA**), which will observe the spectra between 309 nm and 417 nm; The Sunrise Chromospheric Infrared spectroPolarimeter (SCIP, **REFERENCIA**), which will observe the near-infrared; and lastly, the Tunable Magnetograph (TuMag), which will observe three spectral lines in the visible, at 525.02 nm, 525.06 nm and 517 nm.

The design from scratch of an instrument such as this is very complex. There are many things that have to be meticulously designed and tested which span many fields of expertise, like optics, electronics, software, hardware, or thermal design. To avoid undue extension of this thesis, we will focus on the aspects of the design directly related to the **TO QUE**, that is, regarding the spectral, imaging and polarimetric capabilities of the instrument.

1.1 A brief introduction to spectropolarimeters.

Mirar file:///home/pablo/Downloads/s10509-023-04212-3.pdf.

Spectropolarimeters, as suggested by the name, are devices that measure the spectral and polarimetric properties of light, or in other words, that measure the polarization state of light as a function of wavelength. Their use is widely extended in astrophysics due to the huge amout of information about the light source we can infer from these properties.

In solar physics, it is common to encounter two distinct types of spectropolarimeters, distinguished by their approach to spectroscopy: slit-based spectrographs, such as SUSI and SCIP, and narrow-band tunable filtergraphs, like TuMag. The latter preserve spatial resolution by capturing two-dimensional images of the solar scene at the expense of sacrificing spectral resolution. Conversely, slit-based spectrographs provide excellent spectral resolution but have a limited spatial resolution.

Regardless of how spectroscopy is carried out, spectropolarimeters must be able to measure the polarization state of light. That is, they must be capable of determining the Stokes parameters of the incident light. These four parameters, usually grouped in a pseudo-vector: $[I, Q, U, V]$, were defined by Stokes in Stokes (1851) as a mathematical formalism to completely define to polarization state of light. The first parameter, I, represents the total intensity; Q and U provide information about the intensity of linearly-polarized light, at 0° and 90°, respectively; and lastly, V, accounts for the intensity of circularly polarized light.

Excellent polarimetric sensitivity and spectral resolution are wasted if the optical capabilities of the instrument are not up to par. The design of these instruments must achieve diffraction-limited imaging, with a signal-to-noise ratio ensuring a polarimetric sensitivity of 1000 (typically), and the best spatial resolution the telescope allows, all without sacrificing spectral resolution and accomplishing this in the shortest possible time.

When designing the instrument, one must balance these three properties: spectral, optical, and polarimetric capabilities, trying to improve the performance in all of them without sacrificing too much. In the following sections, we will delve into each of these aspects in more detail.

1.1.1 Spectroscopy

Narrow-band tunable spectrographs play a significant role in this thesis. They will be extensively discussed in this chapter, particularly in relation to the design and calibration of TuMag, and again in Chapters 2 and 3 when addressing TuMag's pipeline and the correction of data produced by these instruments. Therefore, for the sake of simplicity, we will focus exclusively on this type of spectrographs from this point onward.

CAMBIAR ESTO.

Fabry-Pérot Interferometers (FPIs), also known as etalons (used interchangeably), represent one of the most prevalent forms of narrow-band tunable spectrographs. Composed by a resonant optical cavity formed by two distinct optical media, these devices allow only the passage of light with wavelengths corresponding to constructive interference within the cavity.

The transmission profile of an etalon, being produced by an interference phenomenon, is characterized by a series of narrow and periodic transmission peaks. The wavelengths at which this resonance peaks are located, their width, and their separation are determined solely by the physical properties of the etalon. In fact, it is not difficult to demonstrate (Bailén et al., 2019) that a resonant cavity produces a periodic transmission profile, with maxima occurring at a wavelength λ such that:

REVISAR -> VÁLIDO PARA TELECENTRIC??

$$\lambda = \frac{2nd\cos\theta}{m}, \tag{1.1}$$

where n is the refractive index of the medium inside the cavity, d is the distance between the mirrors, θ is the angle of incidence of the incoming light ray and m is the interferential order ($m \in \mathbb{Z}$).

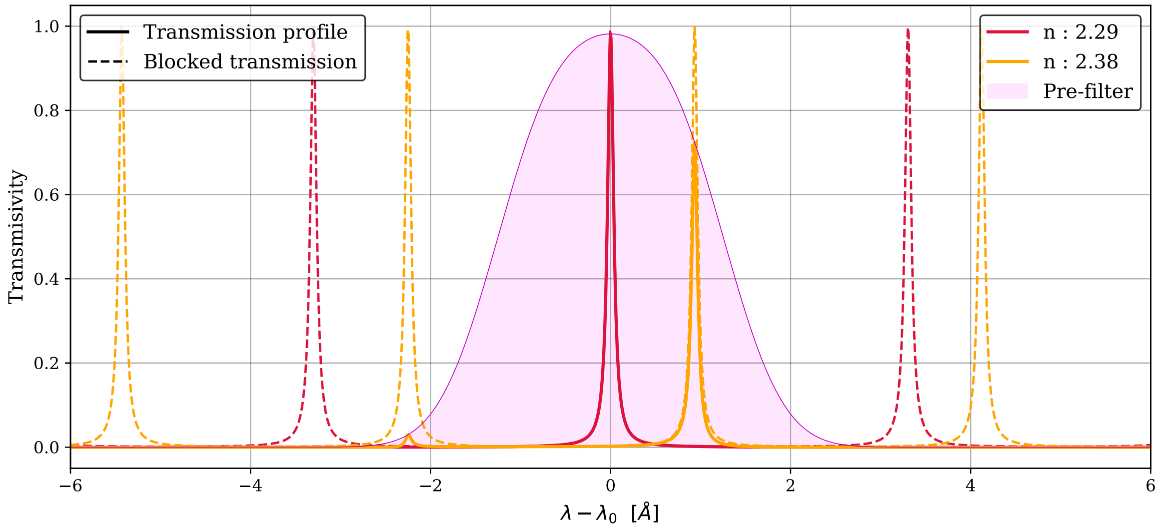

Figure 1.1 Transmission profiles of the same etalon with varying refractive indices (n). The dashed lines represent the original transmission profile, while the solid lines indicate the portion of the transmission profile that passes through the order-sorting pre-filter (shaded purple area).

With Eq. (1.1) in mind, it is clear that an etalon allows for tuning the wavelengths of the transmission peaks by either changing the distance between the mirrors or by altering the refractive index. Although changing the angle of incidence also results in a wavelength shift, it introduces other issues, such as ghost images or profile broadening in telecentric configurations, among other effects. Consequently, the angle is not used for wavelength tuning.

To tune to a single wavelength (or a very narrow band around it), it is necessary to isolate one transmission peak (main order). This is typically achieved by using a pre-filter that only allows light with wavelengths near the desired measurement region to pass through. This ensures that no light reaches the etalon that could pass through it due to interference orders other than the main one (secondary orders).

Figure 1.1 shows a simulation of the spectral behavior of this optical setup. The order-sorting pre-filter is shown with a shaded purple area and the unaltered transmission profile of the etalon is shown in dahsed lines for different values of the refractive index. In solid lines, the resulting transmission profile is shown, that is, the transmission allowed through both the pre-filter and etalon at the same time.

In reality, the spectral and optical properties of FPIs can be quite complex and are influenced not only by their physical characteristics but also by their optical configuration, whether collimated or telecentric. In Chapter 2, we provide a detailed overview of the properties of each configuration, their differences, and the challenges involved in using these devices for data correction.

1.1.2 Imaging

Aquí que va? PSFs Phase diversity?

1.1.3 Polarimetry

XIXA.

Polatimetros, IQUV bien. Etc.

S/N y eficiencia.

1.1.4 What for? Zeeman effect.

1.2 The Tunable magnetograph: TuMag

TuMag is a wavelength-tunable spectropolarimeter capable of probing the line-of-sight velocity ($v$los) and the vector magnetic field ($\vec{B}$) in the photosphere and the low chromosphere. This means that TuMag must be able to switch between different spectral lines and measure the full stokes vector at each observed wavelength.

TuMag's design and properties are a direct consequence of the scientific purpose for which it has been conceived and its requirements.

1.2.1 Optical design and image quality.

1.2.2 Spectral capabilities

As a spectrograph, TuMag is able to tune the wavelength of the measurements through a Fabry-Pérot interferometer (FPI), and select between three different spectral lines through the different pre-filters located on the filter wheel.

The FPI, or etalon, is a $LiNbO_3$-based ...

1.2.3 Polarimetric capabilities

1.3 Calibration of TuMag

Chapter 2

Operation and data reduction.

2.1 TuMag's Pipeline

2.1.1 Darks and flat fields

2.1.2 Blueshift

2.1.3 Demodulation and dual beam

2.1.4 Cross Talk

Chapter 3

Challenges in data reduction: Etalon Cavity Map.

3.1 Cavity map retrieval from flat-field observations

3.1.1 One device, two configurations

file:///home/pablo/Downloads/s10509-023-04212-3.pdf

3.1.1.1 Collimated configuration

Collimated mounts are characterized by having the etalon located at the pupil plane and therefore receive a collimated beam from each point of the observed object. In this setup, light coming from any point of the object will fall upon the same area of the etalon. Consequently, any local defects on the etalon crystals or on the plates' parallelism is averaged all over the clear aperture, thus making the optical quality constant along the FoV. However, the angle of incidence of the light beam varies along the FoV, thus shifting the transmission profile.

The transmission profile for an ideal collimated etalon tuned at wavelength λ_s takes the following form:

$$\Psi^{\lambda_s}(\lambda, \theta) = \frac{1}{1 + F \sin^2 a_s(\lambda, \theta)}, \tag{3.1}$$

where

$$a_s(\lambda, \theta) = \frac{2\pi}{\lambda} n d \cos\theta \ , \tag{3.2}$$

with the subscript s indicating that the etalon is tuned at the wavelength λ_s.

The shape of the transmission profile depends on its physical properties. Firstly, the width of the resonance peaks is determined by the parameter F, $F \equiv 4R(1 - R)^{-2}$, which depends exclusively on the reflectivity R of its mirrors. Secondly, the spectral behavior of the transmission profile is governed by $a_s(\lambda, \theta)$, which is a function of the refractive index of the etalon cavity, n; the distance between mirrors, d; and the angle of the incident beam, θ.

Local defects in the collimated configuration are averaged out, which means that d and n respectively represent the mean values of the thickness and refractive index across the clear aperture of the FPI. Yet, they produce a broadening of the transmission profile and worsen the optical quality of the instrument. The differing angles of incidence over the FoV produce shifts of the transmission that vary quadratically with θ.

3.1.1.2 Telecentric configuration

In the telecentric configuration, the etalon is placed very close to an intermediate focal plane, while the pupil is focused at infinity. This way, the etalon is illuminated by cones of rays that are parallel to each other and reach different sections of the interferometer. Local inhomogeneities (defects or cavities) on the etalon produce differences in the transmission profile across the FoV, which are directly mapped into the image plane. This means that the optical response and the transmission profile shift locally on the image sensor.

The transmission profile of the etalon tuned at a wavelength λ_s is, in this case, given by (Bailén et al., 2021):

$$\Psi^{\lambda_s}(\lambda) = \mathfrak{Re}\left[E(a_s(\lambda, n, d, \theta), b)\right]^2 + \mathfrak{Im}\left[E(a_s(\lambda, n, d, \theta), b)\right]^2, \tag{3.3}$$

with $E(a, b)$ being:

$$E(a,b) = 2\sqrt{\tau}\left\{\int_0^1 \frac{\varrho\cos\left(a\left[1-b\varrho^2\right]\right)}{1+F\sin^2\left(a\left[1-b\varrho^2\right]\right)}\mathrm{d}\varrho + \mathrm{i}\frac{1+R}{1-R}\int_0^1 \frac{\varrho\sin\left(a\left[1-b\varrho^2\right]\right)}{1+F+\sin^2\left(a\left[1-b\varrho^2\right]\right)}\mathrm{d}\varrho\right\}, \tag{3.4}$$

where τ is the transmission factor of the etalon at normal incidence, ϱ is the radial coordinate of the pupil normalized to the pupil radius of the instrument, a is defined by Eq. (3.2) and b is given by

$$b = \frac{1}{8(nf\#)^2}. \tag{3.5}$$

This parameter accounts for the contribution of the focal ratio, $f\#$, and has an impact on the spectral resolution and the apodization of the pupil as seen from the etalon (Beckers, 1998). Thus, the resolution is now affected by both F and $f\#$, through the parameters a and b.

Contrary to the collimated case, a now has an explicit dependence on the spatial coordinates of the image plane, as n and d change from pixel to pixel. These variations compose the "cavity error" of the etalon and need to be corrected when employing telecentric configurations.

3.2 Sunspot observation simulation.

Chapter 4

Summary and conclusions

The conclusions are …

Appendix A

Profile derivatvies

Bibliography

Bailén, F. J., Suárez, D. O., & del Toro Iniesta, J. On fabry–pérot etalon-based instruments. i. the isotropic case. *The Astrophysical Journal Supplement Series* **241**, 9 (2019).

Bailén, F. J., Suárez, D. O., & del Toro Iniesta, J. On fabry–pérot etalon-based instruments. iv. analytical formulation of telecentric etalons. *The Astrophysical Journal Supplement Series* **254**, 18 (2021).

Beckers, J. On the effect of narrow-band filters on the diffraction limited resolution of astronomical telescopes. *Astronomy and Astrophysics Supplement Series* **129**, 191 (1998).

Stokes, G. G. On the composition and resolution of streams of polarized light from different sources. *Transactions of the Cambridge Philosophical Society* **9**, 399 (1851).

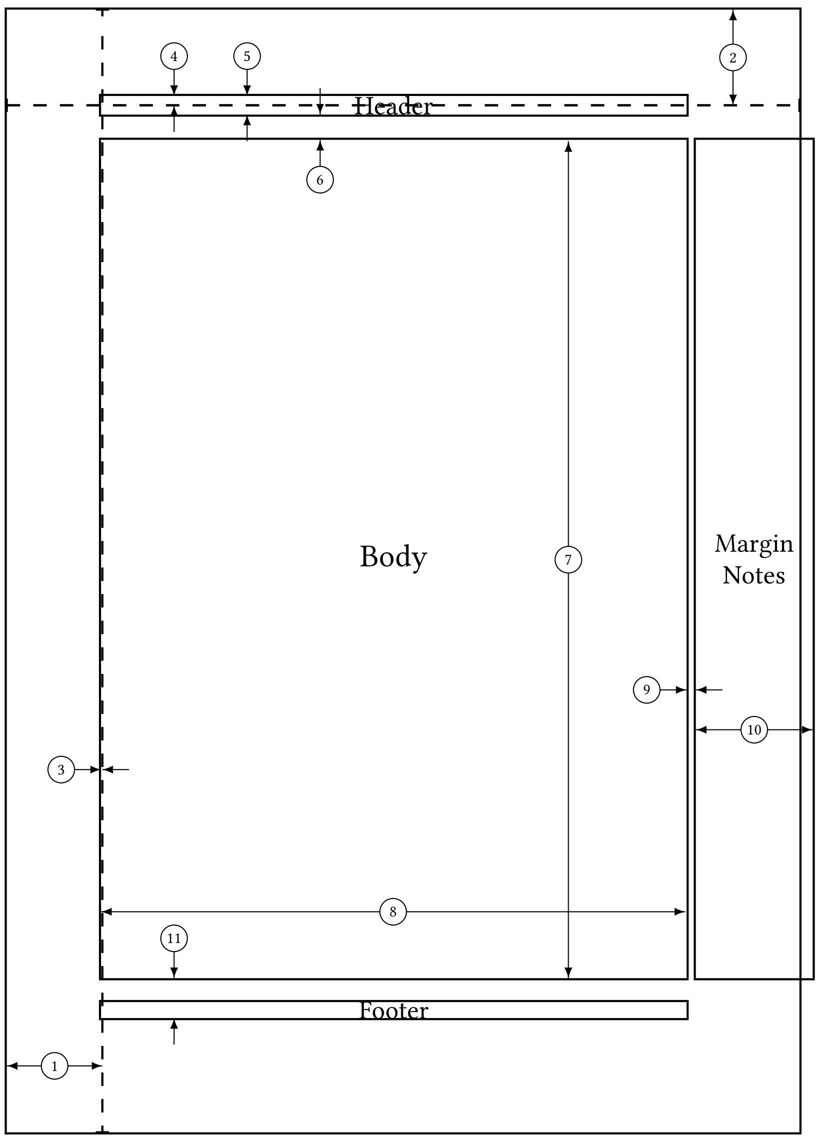

1	one inch + \hoffset	2	one inch + \voffset
3	\oddsidemargin = -1pt	4	\topmargin = -7pt
5	\headheight = 14pt	6	\headsep = 19pt
7	\textheight = 631pt	8	\textwidth = 441pt
9	\marginparsep = 7pt	10	\marginparwidth = 88pt
11	\footskip = 30pt		\marginparpush = 7pt (not shown)
	\hoffset = 0pt		\voffset = 0pt
	\paperwidth = 597pt		\paperheight = 845pt

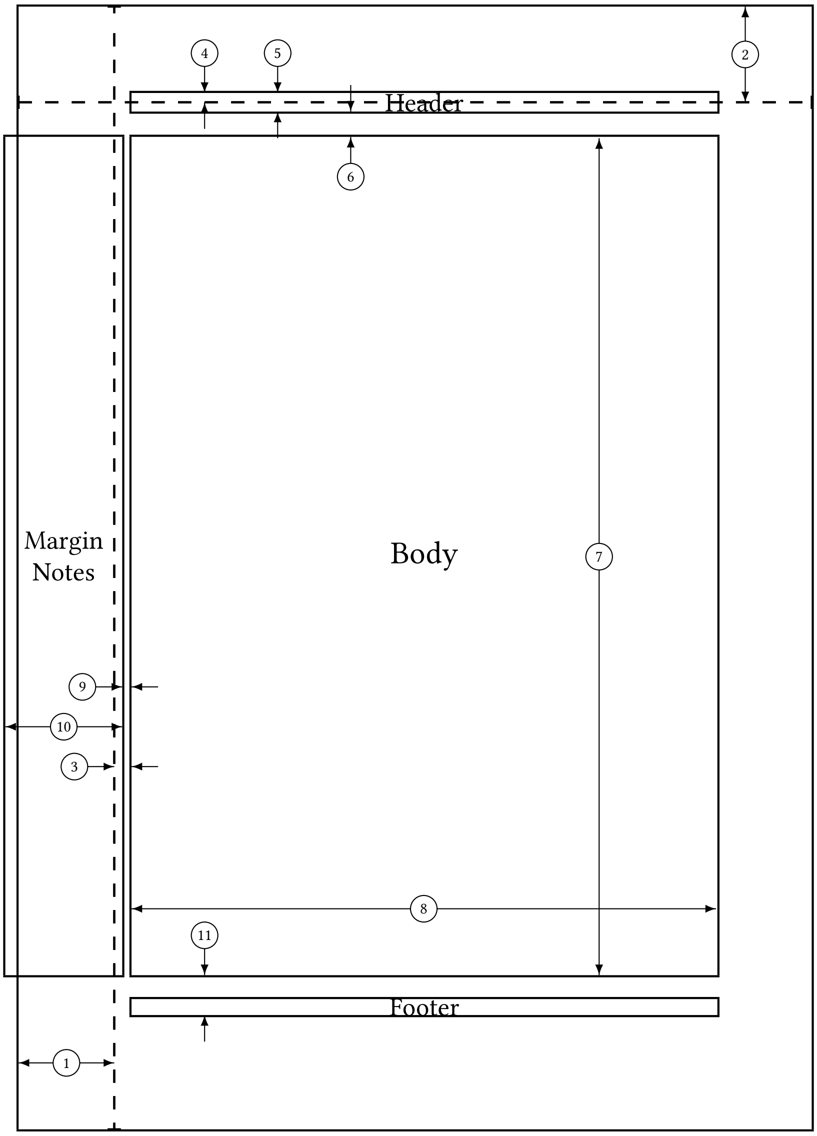

1	one inch + \hoffset	2	one inch + \voffset
3	\evensidemargin = 13pt	4	\topmargin = -7pt
5	\headheight = 14pt	6	\headsep = 19pt
7	\textheight = 631pt	8	\textwidth = 441pt
9	\marginparsep = 7pt	10	\marginparwidth = 88pt
11	\footskip = 30pt		\marginparpush = 7pt (not shown)
	\hoffset = 0pt		\voffset = 0pt
	\paperwidth = 597pt		\paperheight = 845pt